CHAPTER 2 LITERATURE REVIEWS

2.1 Porous Materials

A porous medium is a material that is a solid matrix with an interconnected void structure. The porous media examples are wood, human lung, sponge, and sand stone (Fig. 2.1). The general porous media using in combustion are SiC, Al_2O_3, ZrO_2 and YZA as shown in Fig.2.2. It should have high temperature resistance material and longer durability suffers from cracking due to the differential expansion stress experienced during startup and shutdown. A large number of researches in field of porous media are reported however this chapter presents the overview of porous media in combustion applications.

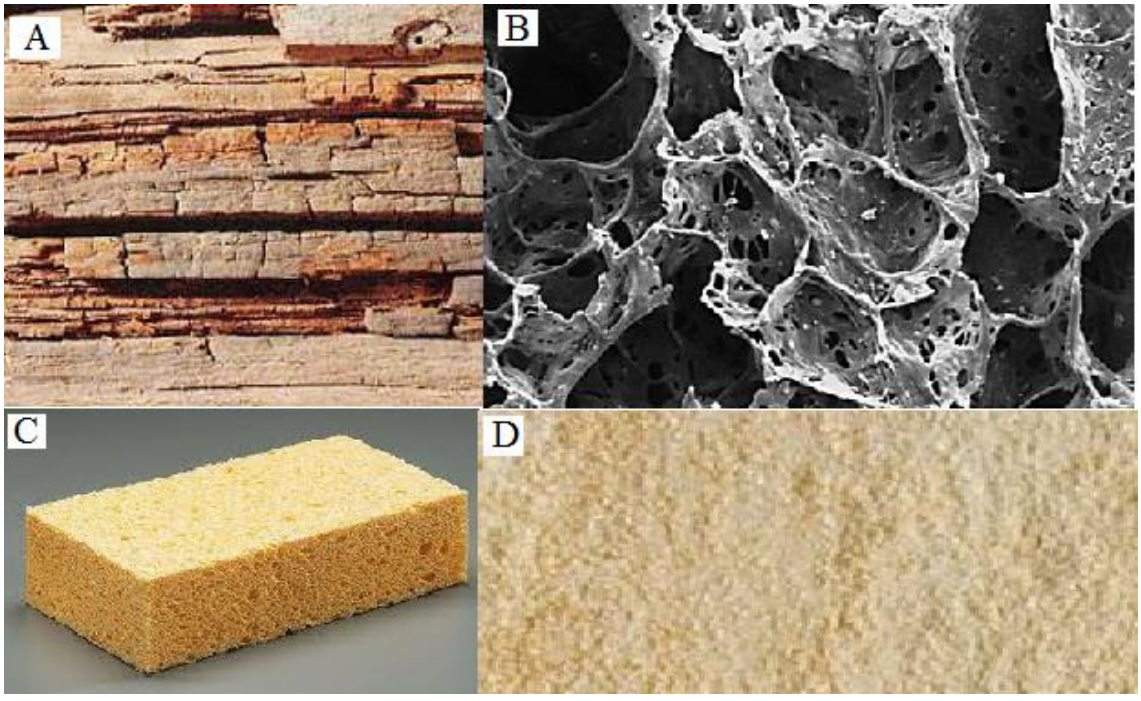

Figure 2.1 The porous materials type: A) wood, B) human lung, C) sponge and D) sandstone.

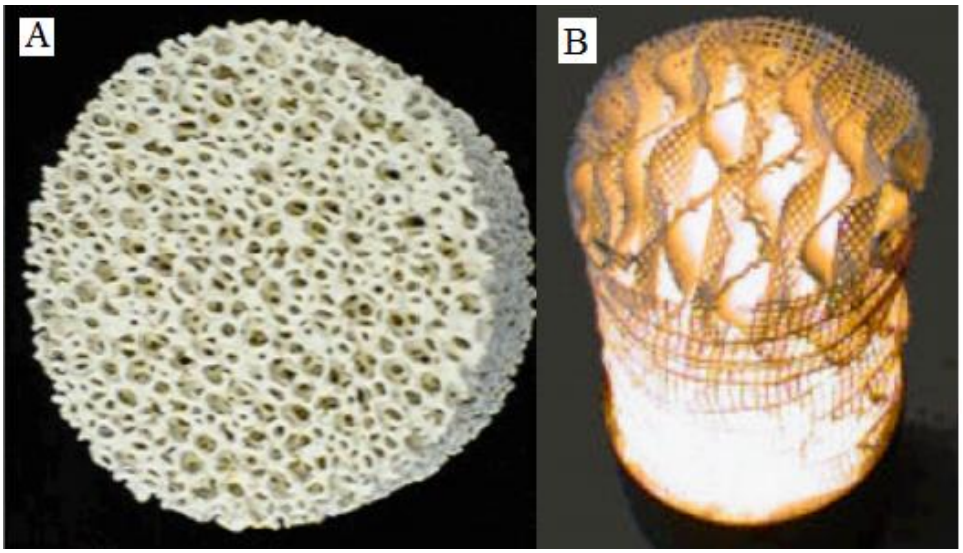

Figure 2.2 Examples of porous structures: A) Reticulated foam made of ZrO_2 and B) Lamella structure made of Al_2O_3 fibbers.

A combination between base material type and porous structure is very important to porous burner design to determine the combustion performance, the longevity and the system's versatility (Tierney and Harris, 2009). Ceramic materials are popularity used as porous burner because ceramic materials have a good temperature resistance; their durability suffers from cracking caused by the stresses of differential expansion experienced during startup and shutdown (Howell et al., 1996). Alumina oxide (Al_2O_3), zirconia oxide (ZrO_2), and silicon carbide (SiC) are the main based-materials types are used. Other ceramics and high-temperature metals have only been occasionally employed (Tierney and Harris, 2009). All porous materials based are substantially different with regard to manufacturing and properties. The lists of important data for these materials are shown in table 2.1.

Aluminum oxide (Al_2O_3, alumina, corundum) is a chemical compound and consists of aluminum and oxygen. This have been utilized as the inorganic chemical for ceramics and produced from the mineral bauxite via the Bayer process (Carter and Norton, 2007). Al_2O_3 is often used in combustion applications because of its high hardness, high chemical resistant, and high temperature resistant. Alumina-based materials have the intermediate thermal conductivity, thermal expansion resistance to thermal shock, and overall emissivity. Presently, Al_2O_3 is the lowest-cost and high performance ceramic because the large production volume (Scheffler and Colombo, 2005). Moreover, Al_2O_3

has been employed in a variety of porous structures, i.e. packed bed of Al_2O_3 ball, cellular foams, and fiber lamellae.

Table 2.1 Important properties of Al_2O_3, SiC, and ZrO_2 (Scheffler and Colombo, 2005).

Property	**Unit**	**Al_2O_3**	**SiC**	**ZrO_2**
Maximum use temperature in air	^oC	1900	1650	1800
Thermal expansion coefficient (20-1000 ^oC)	10^{-6} K^{-1}	8	4-5	10-13
Thermal conductivity at 20 ^oC	W m^{-1} K^{-1}	20-30	80-150	2-5
Thermal conductivity at 1000 ^oC	W m^{-1} K^{-1}	5-6	20-50	2-4
Specific thermal capacity	J g^{-1} K^{-1}	0.9-1	0.7-0.8	0.5-0.6
Thermal stress resistance parameter, hard shock, R (σ/Eα)	K	100	230	230
Thermal stress resistance parameter, mild thermal shock, R' (Rλ)	10^{-3} W m^{-1}	3	23	1

Zirconium dioxide (ZrO_2, zirconia) is principally derived from zircon, ZrSiO4, which occurs in igneous rocks such as granites and pegmatite (Carter and Norton, 2007). ZrO_2 is an inorganic metal oxide that is mainly used in ceramic materials. Zirconia-based materials show excellent high temperature resistance with low thermal conductivity and thermal shock resistance. Recently, the uses of zirconia media in recent porous burner applications was limited due to the poor heat transport and thermal shock resistance, (Tierney and Harris, 2009).

Silicon carbide (SiC) is a chemical produced from the one-to-one binding of carbon (C) and silicon (Si), and is the most widely used as non-oxide ceramic. Its major application is in abrasives due to its hardness. Silicon carbide does not occur in nature and therefore must be synthesized (Carter and Norton, 2007). SiC-based materials can be used at a maximum temperature of approximately 1650 ^oC that is higher resistant to chemical corrosion, such as oxidation, than other non-oxide ceramics. These consequently used for crucibles, parts for kiln burning, mechanical seals, and parts materials to produce

semiconductors. Silicon carbide has a high thermal conductivity, low thermal expansion, and good resistance to thermal shock (Scheffler and Colombo, 2005).

2.2 Porous Structures

2.2.1 Discrete elements

A number of porous burners were investigated by the discrete elements making up a packed bed. The advantage of discrete elements over cellular structure is quite durable due to they are not constrained in a rigid matrix, but they have a robust shape. The main discrete element media used in burner research are ceramic balls, ceramic pebbles and ceramic saddles (Tierney and Harris, 2009). A packed bed of uniform diameter spheres typically has porosity in the range of 0.2595 to 0.4764 (Nield and Bejan, 2006). The discrete element media are shown in Figure. 2.3

Figure 2.3 Discrete element: A) Ceramic balls, and B) Ceramic pebbles, and C) Ceramic saddles.

2.2.2 Cellular structures

Cellular ceramics, namely, ceramic foams or porous ceramics which offer a series of unique properties because of the combination of highly porous cellular structure and tailored composition of strut material. The ceramic foams are manufactured in variation shapes, for instance honeycombs, lamellar structure and reticulated ceramic foam as shown in figure 2.4. The Ceramic foams have been widely used in porous burners due to a good conductivity heat transport, the lower macroporosity lead to a rather long start-up phase, intermediate radiative heat-transport properties, intermediate dispersion properties, and relatively high pressure drop (Scheffler and Colombo, 2005).

The general monolithic structures have low porosity, low thermal conductivity and limited radiative heat transfer. Therefore the monolithic structure is suitable for the preheat zone of a porous burner because this can be reduced the risk of flame flashback (Tierney and Harris, 2009).

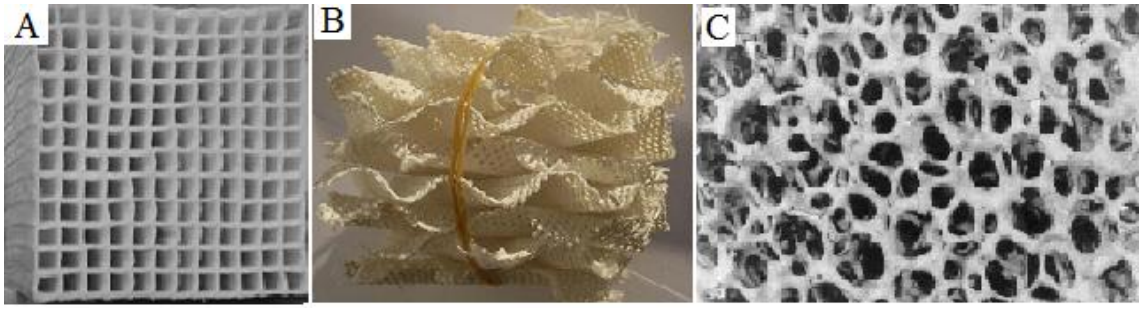

Figure 2.4 Porous ceramics: A) Honeycomb shape, and B) Lamellar structure, and C) Reticulated ceramic foam.

2.3 Porous properties

2.3.1 Porosity

The porosity of a porous medium (ε) is defined as the fraction of the total volume of the medium that is occupied by void space (Nield, 2006) or the porosity is the volumetric void fraction of the material (Howell et al., 1996). In the other word, the porosity is the pore volume divided by the total volume occupied by the porous medium. Thus 1-ε is the fraction that is occupied by solid. The porosity is a main physical property of the porous medium that affects mechanical and thermal properties. In additions, there are many correlations such as effective thermal conductivity, volumetric heat transfer coefficient, elasticity, and pressure drop of porous medium are commonly based on the porosity.

The surface porosity, which is the fraction between void area and total area of a typical cross section, will normally be equal to ε for an isotropic medium. The porosity of general media is less than 0.6, if the packed beds consist of uniform diameter solid spheres, ε is in the range between 0.2595 (rhombohedral packing) and 0.4764 (cubic packing). The porosity of non-uniform grain size are smaller than the uniform grains

due to the smaller grains are fill the pores and formed to larger grains. For man-made material materials ε can approach value 1. For example, the porosity of Al_2O_3 fiber lamellae and SiC porous foam were used 0.9, which defined by Pereira et al. (2010).

The porosity of porous medium can be measured by dividing the total volume of water extruded from a solid within porous structure as shown by equation 2.1.

$$\text{Porosity} = \text{volume of water/volume of porous.} \qquad (2.1)$$

Moreover, the porosity is also predicted by numerical method. The correlations to predict the variation in porosity of a packed bed were reviewed by Van Antwerpen et al. (2010).

For non-uniform porosity porous medium, the total medium volume is simply defined as the sumation of volumes of cells as shown in Figure 2.5. Thus, the porosity is following equation 2.2 (Liou, 2005)

$$\varepsilon = \frac{\sum_{i=1}^{n_{fluid}} V_i}{\sum_{i=1}^{n_{total}} V_i}. \qquad (2.2)$$

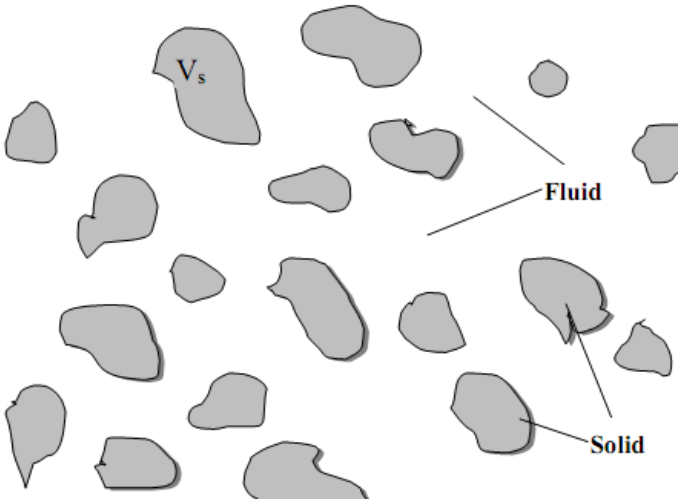

Figure 2.5 non-uniform porous medium.

2.3.2 Thermal conductivity

Fourier's law explains heat conduction in a medium. This law describes that heat transport is proportional between the thermal conductivity and the temperature gradient:

$$\dot{q} = -\lambda \nabla T \tag{2.3}$$

Where $\dot{q}$ = heat flux density (heat per unit time and unit area), W m^{-2}, and

T = the temperature, K

In porous structure, the thermal conductivity is not a homogenous material property. The thermal conductivity is more complicated than pure solid or fluid phase. It is a combination of several different mechanisms taking place at the pore-size level i.e. heat conduction through the solid walls, heat conduction in the fluid, and radiative heat transfer. Heat transfer problems within porous media also complicated. An "effective thermal conductivity" λ_{eff} has been introduced to simplify the calculations. The porous material is assumed as a "black box" and "local thermal equilibrium". Then, the solution of the equations by Fourier's law is still possible:

$$\dot{q} = -\lambda_{eff} \nabla T \tag{2.4}$$

The overall thermal conductivity of porous medium depends on the complex geometry structure. The porous media consist of solid and fluid void, which affect thermal conductivity of material. The effective conductivity of porous media is focused in two approaches, which are the conductivity effect neglecting and accounting for radiation.

Most of the theoretical correlations were developed to predict the effective thermal conductivity by considering the idealization of unidirectional heat transfer or two-dimensional heat flow. At the low temperature porous medium, the radiation has no significant contribution to the overall heat transfer rate. The practical models to predicting the stagnant effective thermal conductivity are the parallel and series models (Combarnous and Bories, 1975). If the heat conduction in solid and fluid phases is considered in parallel, then the overall conductivity, λ_A is the weighted arithmetic mean of the solid (λ_s) and fluid (λ_f) conductivities.

$$\lambda_A = (1- \varepsilon)\, \lambda_s + \varepsilon\lambda_f. \quad \text{(Parallel-weighted arithmetic mean)} \qquad (2.5)$$

When the heat conduction of solid and fluid phases has been considered in series, the overall conductivity (λ_A) is the weighted harmonic mean of λ_s and λ_f:

$$\frac{1}{\lambda_A} = \frac{1-\varepsilon}{\lambda_s} + \frac{\varepsilon}{\lambda_f} \qquad \text{(Series-weighted harmonic mean)} \qquad (2.6)$$

The parallel model is suitable for the λ_s and λ_f in the same magnitude, i.e., their ratio is close to unity (Prasad et al., 1989). Some correlations to predict the effective thermal conductivity of packed bed are listed in table 2.2.

At high temperature shows the contribution of heat radiation within the pore to the effective thermal conductivity of the medium is dominated. In additions, the effective thermal conductivity accounting for radiation is a main parameter to simplify governing equation of heat transfer in porous medium problem. The radiation term in solid phase energy equation is an extremely non-linear term. The radiation term is transformed into conduction term by using effective conductivity accounting for radiation, thus the solid equation will be linear equation, and the analytical solution can be created.

Besides to predict the effective thermal conductivity by theoretically approach, the experimental methods can be also used to find this quantity. The hot-plate method is used to examine the thermal conductivity in case of without heat flow. A temperature gradient inside the experimental body generates a one-dimensional heat flow in the measurement area. Then, the effective thermal conductivity λ_{eff} (W/m.K) can be calculated via following equation

$$\lambda_{eff}(T) = \frac{\dot{q}.s}{\Delta T}. \qquad (2.7)$$

The photograph and schematic diagram of experimental was shown in Fig. 2.6 (Scheffler and Colombo, 2005). Becker et al. (2003) presented the thermal conductivity

of various ceramic foam materials. The results shown that the thermal conductivity significantly increases with temperature (Fig. 2.7)

Table 2.2 The effective thermal conductivity correlation.

References	The effective thermal conductivity correlation
Licheneker, K. (1926)	$\lambda_{eff} = \lambda_f^{\varepsilon}.\lambda_s^{(1-\varepsilon)}$
Kunii, D. and Smith, J. M. (1960)	$\lambda_{eff} = \lambda_f.\left[\varepsilon + \frac{\beta.(1-\varepsilon)}{\Psi + \gamma.\left(\frac{\lambda_f}{\lambda_s}\right)}\right]$ Where the empirical value $\beta = 0.895$ for a close packing of spheres and $\beta = 1$ for a loosely packed bed. The empirical values $\gamma = 2/3$ and empirical constant Ψ is a function of the number of contacts responsible for heat transfer.
Krupiczka (1967)	$\lambda_{\mathbf{eff}} = \lambda_{\mathbf{f}}.\left(\frac{\lambda_{\mathbf{s}}}{\lambda_{\mathbf{f}}}\right)^{\mathbf{n}}$ Where $n = 0.280 - 0.757\log_{10}\varepsilon + 0.057\log_{10}\left(\lambda_f/\lambda_s\right)$
Zehner, P. and Schlünder Schlunder, E., U., (1970)	$\lambda_{eff} = \lambda_f.\left\{1-\sqrt{1-\varepsilon} + \frac{2\sqrt{1-\varepsilon}}{1-\kappa^{-1}B} \times\left[\frac{\left(1-\kappa^{-1}\right)B}{\left(1-\kappa^{-1}B\right)^2}\ln\left(\frac{1}{\kappa^{-1}B}\right) - \frac{B+1}{2} - \frac{B-1}{1-\kappa^{-1}B}\right]\right\}$ Where $B = 1.25[(1-\varepsilon)/\varepsilon]^{10/9}$ and $\kappa = \lambda_s/\lambda_f$.

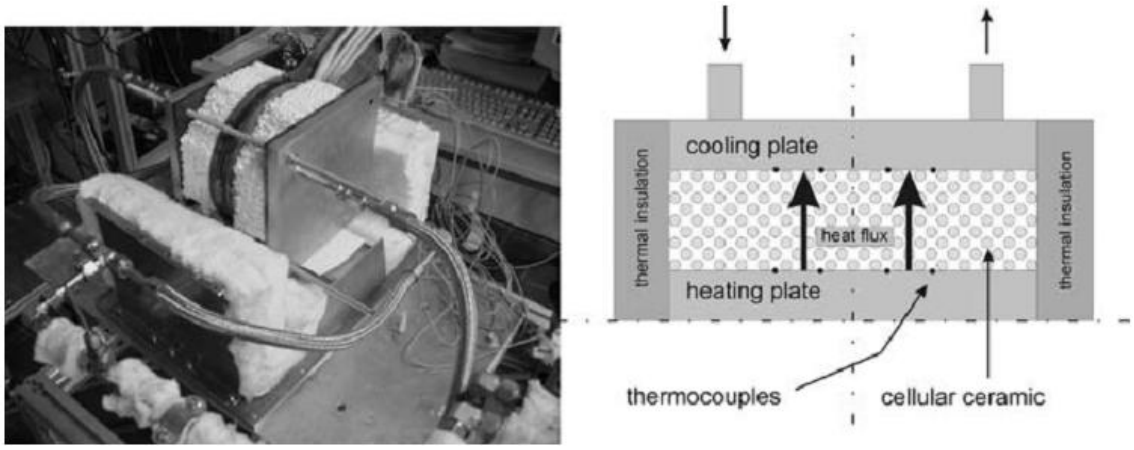

Figure 2.6 Photograph and schematic diagram to measure thermal conductivity without heat flow by the hot-plate method (apparatus built at the Institute of Fluid Dynamics, Friedrich Alexander University of Erlangen-Nuremberg).

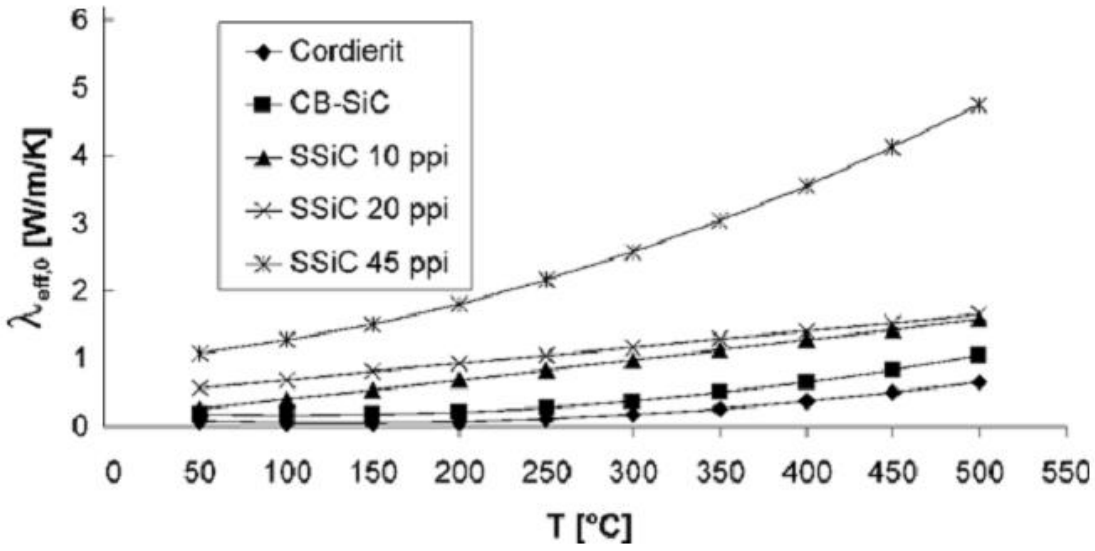

Figure 2.7 Thermal conductivities without flow of various ceramic foam materials with porosity of 0.76 determined by the hot plate method (Becker et al., 2003).

The phenomena of heat conduction in the fluid, heat conduction in the solid, convective heat transfer, and radiative heat transfer are considered separately lead to the heat-transfer calculations are complicated. The effective thermal conductivity can be simplified the calculation. However, the calculation by using the effective thermal conductivity cannot elucidate in each heat transfer mechanisms and cannot indicate each

quantity of heat transfer mechanisms. Therefore, in this thesis, all mechanisms of heat transfer are separately considered by using the governing equation in order to intensively understand.

2.3.3 Heat transfer coefficient

The porous medium are heated or cooled by a fluid flows through the medium hence the different between fluid and solid temperatures that is a heterogeneous approach problems. The convective heat transfer between fluid and solid phases are also occurs.

In general, the convective heat transfer coefficient is determined by three ways, which are the theoretical data, experimental based and semi-empirical method. The exact mechanism by which the heat transfer coefficient within porous media is far from clear. Because the porous configuration that have complex and the surface to volume ratio is very difficult to predict or investigate. The heat transfer coefficient between solid and fluid phases within porous media is usually presented in terms of volumetric coefficient (the heat transfer per degree of temperature difference per unit volume of porous material). The convective heat transfer between fluid and liquid phases is defined by the following equation:

$$\dot{q}_v = \alpha A_v (T_s - T_F). \tag{2.8}$$

Where $\dot{q}_v$ = the volumetric heat flow [W/m^3],

α = the convective heat transfer coefficient [$W/m^2.K$],

A_v = the specific surface area to volume ratio [m^2/m^3],

T_s = the solid temperature [K], and

T_F = the fluid temperature [K].

The convective heat transfer of porous materials are usually presented in terms of a volumetric heat transfer coefficient,

$$h_v = A_v \alpha. \tag{2.9}$$

The correlation to predict volumetric heat transfer coefficient usually report as the volumetric Nusselt number (Nu_v) and the Reynolds number (Re). Maiorov (1978) proposed the correlation of sintered metals as following

$$Nu_v = \frac{h_v l_c^2}{k} = C(Re.Pr)^m, \tag{2.10}$$

where l_c = the characteristic length-scale, and $0.65 < m < 1.84$.

Wakao and Kaguei (1979) performed the experimental to determine the dimensionless correlation for the convective heat transfer coefficients. The relationship is performed for bed packing for Re > 10. The particle diameter is used as the characteristic length. The correlation as shown by equation 2.9.

$$Nu_v = 2.0 + 1.1 Re^{0.6} Pr^{1/3}. \tag{2.9}$$

The correlation for lower and higher Reynolds number ranges with flow through the spherical particles packed beds was proposed by Achenbach (1995). The correlation is suitable for air (Pr = 0.71), the packed bed with porosity of 0.387, and 1 < Re/porosity < 7.7×10^5. The correlation as following;

$$Nu_v = \left\{ \left(1.18 Re^{0.58}\right)^4 + \left[0.23 \left(Re/\varepsilon \right)^{0.75} \right]^4 \right\}^{1/4}. \tag{2.10}$$

Galitseysky and Mozhaev (1993) reported a semi-empirical correlation for high density porous materials that is valid for the form of 10 < Re < 500 (Eq.2.11)

$$Nu_v = A\left[\varepsilon (1-\varepsilon)^3 \right]^{0.5} Re.Pr \tag{2.11}$$

Where $A = f(L/d_m)$ can be determined from the experimental data. For mullite, the experimental data obtained $A = 37.2/ (L/d_m) - 0.59$. The correlation is valid for L/d_m range between 4.35 to 6.67 range and Re.Pr range between 17 to 582.

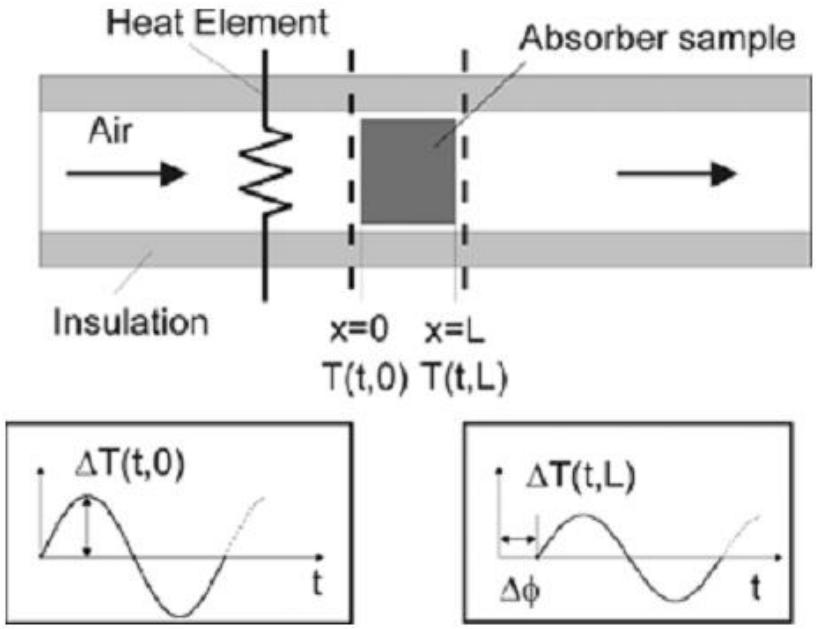

Figure 2.8 Experimental setup for measuring convective heat transfer properties of cellular materials (Viskanta and Younis, 1993).

Viskanta and Younis (1993) measured the heat-transfer coefficient by using experimental based as shown in Figure 2.8. The air was heated by an electrically heating element before flows through porous sample. The tube also was insulated in order to keep the air temperature constant. The air temperature shown as a temperature wave T(t,x), where x is the air flow direction. The amplitude and the frequency of the temperature wave can be controlled. The air temperature was monitored at the inlet and outlet of the airflow through the sample. An attenuation of the temperature wave and a phase shift $\Delta\phi$ is induced by the porous sample. Thus, the product of the specific surface area A_v and the heat transfer coefficient can be calculated (Hoffschmidt et al., 1997).

Fend et al. (2004) was investigated convective heat transfer in ceramic foam materials. The cordierite, clay-bound silicon carbide (CB-SiC), and sintered silicon carbide (S-SiC) foam materials were studied. The volumetric heat transfer coefficient αA_v as a function of fluid velocity for 20 ppi materials with a porosity of 0.76 as shown in Fig. 2.9. The graph illustrated that for αA_v is increased with higher fluid velocity for all porous materials. The different type of porous materials have no significantly affect to αA_v.

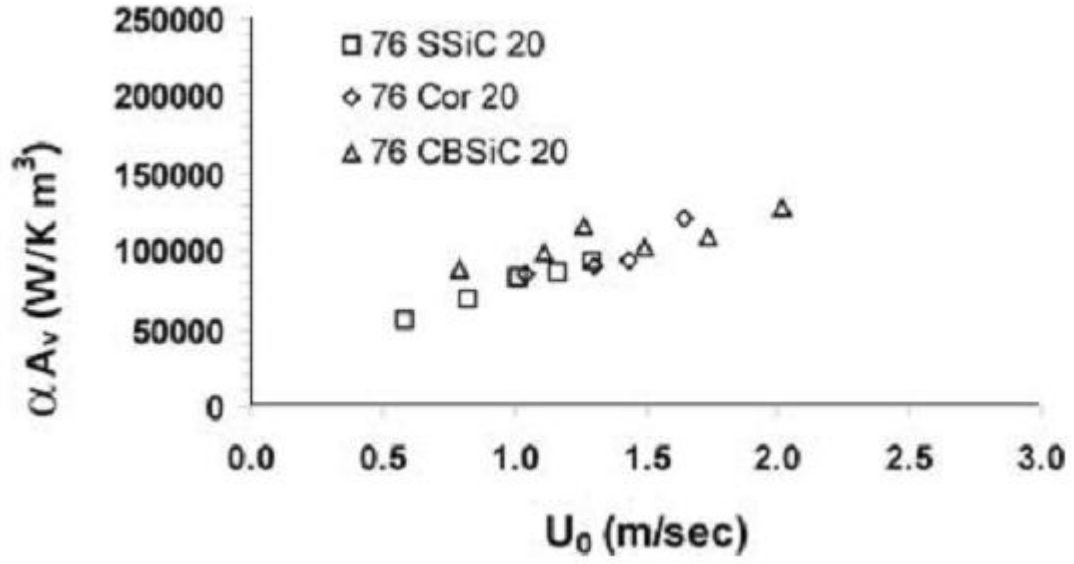

Figure 2.9 Volumetric heat transfer coefficients of various 20 ppi ceramic foam materials with 76% porosity (Fend et al., 2004).

The available correlations and theoretical approaches for predicting the heat transfer coefficient in porous materials were reviewed by Viskanta (1995) and Nield and Bejan (2006).

Although the many group of researchers have been studied the physical properties of various porous materials, however the correlation for the numerical model should be based on the model validation with the experimental due to the complex structure of porous materials. Therefore, the suitable correlation for each model should be employed the collect result with the experimental.

2.4 State of modeling of combustion within porous media

To date, the several methods have been proposed as a way for advance free flame combustion technology. A premixed combustion within porous media are seen the main candidate for this technology in order to the higher heat recirculation between solid to solid phase conduction and radiation compared with the flowing gas. Burners having heat recirculation provide higher thermodynamic efficiencies and flame temperature (Hardesty and Weinberg 1974). Many studies show that the porous burner can unlock the limitation of conventional burner due to it provide high radiant efficiency with low

hazardous emission (e.g. NO and CO). The literature review is conducted and grouped in the following parts: combustion modeling of gaseous fuel within porous media, combustion modeling of liquid fuel within porous media.

The combustion within porous media was studied for both experimental and modeling. The limitations of measurement equipment (e.g. mechanical probes and optical instruments) are the main problems for experimental. Moreover, the experimental research has high cost and required the long time period in operation. The modeling is challenging because of unlocking limitation of experiment and clarifies the new knowledge in term of the thermal fundamentals. Earlier models simply assumed that the gas and solid phase were in local thermal equilibrium. The previous research groups (Chen et al. (1987), Sathe et al. (1990), Hsu el al. (1993) and Yoshizawa et al. (1988)) are developed numerical modeling. The large volumetric heat transfer coefficient has been assumed, thus the gas and solid temperature could be assumed to be the same.

Yoshizawa et al. (1988) have investigated a one-dimensional analytical premixed combustion model in a porous medium burner. The burner has fixed length and consists of fine particles dispersed homogeneously. The assumptions introduce in this model are constant physical properties, one-step reaction and steady state approach. Solid and gas phase conduction, solid radiation, and heat exchange between the solid and the gas phases were also considered. The results confirmed that the combustion in a porous medium is excess enthalpy flames. At the same mixture, the flame temperatures of the porous burner are higher than the corresponding adiabatic flame temperature. Moreover, the porous burner has higher flame speed than the open flame. The study concluded that radiation is more important than solid conduction in excess enthalpy burning.

Tong and Sathe (1990) developed a one-dimensional conduction, convection and radiation model. The combustion model was assumed heat generation. The gas and solid phases energy equations were considered separate. The solid matrix was assumed to emit, absorb, and scatter radiant energy, and the spherical harmonics approximation was used to solve the radiative transfer equation. The results shown that for a given rate of heat generation, large optical thicknesses and high volumetric heat transfer coefficients were desirable for maximizing the radiant output.

Sathe et al. (1990) proposed an experimental and theoretical study of porous radiant burner performance of premixed between methane and air. The model considered a 1-D laminar premixed flame and one step reaction combustion. The results indicated that stable combustion at elevated flame speeds could be maintained in two different spatial domains: one spanning the upstream half of the porous region and the other in a narrow region near the exit plane. In the upstream region, the combustion zone moved to downstream as the higher flame speed. In additions, the flame speeds were greater than the laminar flame speed. The heat release and the radiant output increased as the flame zone was shifted towards the middle of the porous layer. This was due to lower upstream heat losses and higher heat release rates.

Henneke and Ellzey (1999) developed a one-dimensional model to investigated the low-velocity filtration combustion reaction of lean methane/air mixtures in packed bed. The burner geometry is shown in Fig. 2.10. The model considered gas-phase transport, radiation, interphase heat exchange, and solid conduction. The reaction was represented with a complete methane/air kinetics mechanism. The results indicated that gas phase dispersion has significantly affects on the wave speed only at higher equivalence ratios. In addition, the predicted solid temperature matched with experiments for a mixture with an equivalence ratio of 0.15. Over a wide range of equivalence ratios, the computed show the same trends but higher on wave speeds compared with the theoretical predictions.

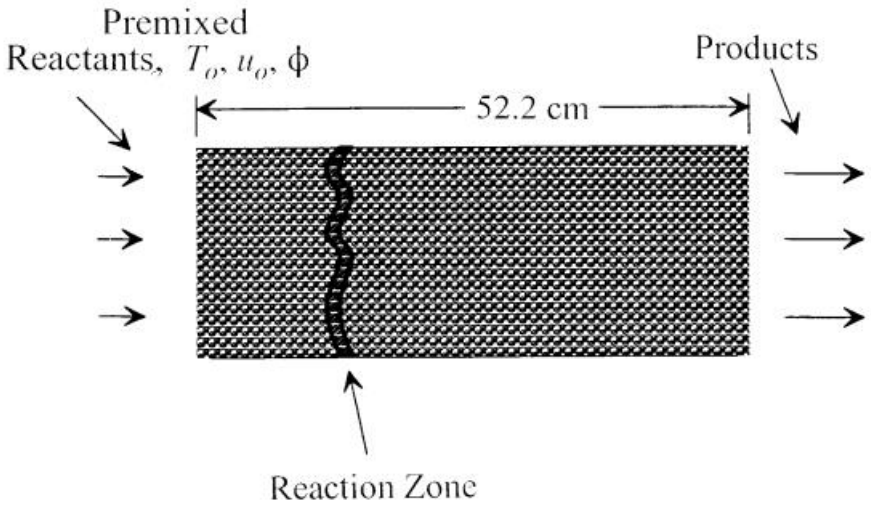

Figure 2.10 Single-layer porous burners (Henneke and Ellzey, 1999).

In previous works have indicated that the PMB provides higher flame speed than free flame due to the hampers flame stabilization in porous media. For solving the task of flame stabilization in porous media, Trimis et al. (1996) proposed a principle for flame stabilization by using thermal flame quenching. The bi-layered porous burner, which combines of two regions with different pore sizes, was carried out. This principle is shown in Figure 2.11. The upstream porous section has a small-pored which the combustible gas is preheated, while the downstream porous section is a large-pored for combustion process. The deciding factor to specify flame able or unable to propagate is the Peclet number or Pe, which is defined as following equations,

$$Pe = (S_L d_m C_p \rho)/k \tag{2.12}$$

Where S_L is the laminar flame speed, d_m is the equivalent diameter of the average hollow space in porous medium. The C_p, ρ, and k are the specific heat, the density, and the thermal conductivity coefficient of the gas mixture, respectively. If Pe < 65, the flame is quenched or unable to propagate, since heat is transferred to the porous medium at a higher rate than it was production. On the other hand, Pe > 65 shows the flame is able to propagate or the combustion can be occurred. Thus, the Pe of upstream porous layer should less than 65. The downstream porous layer should have Pe > 65.

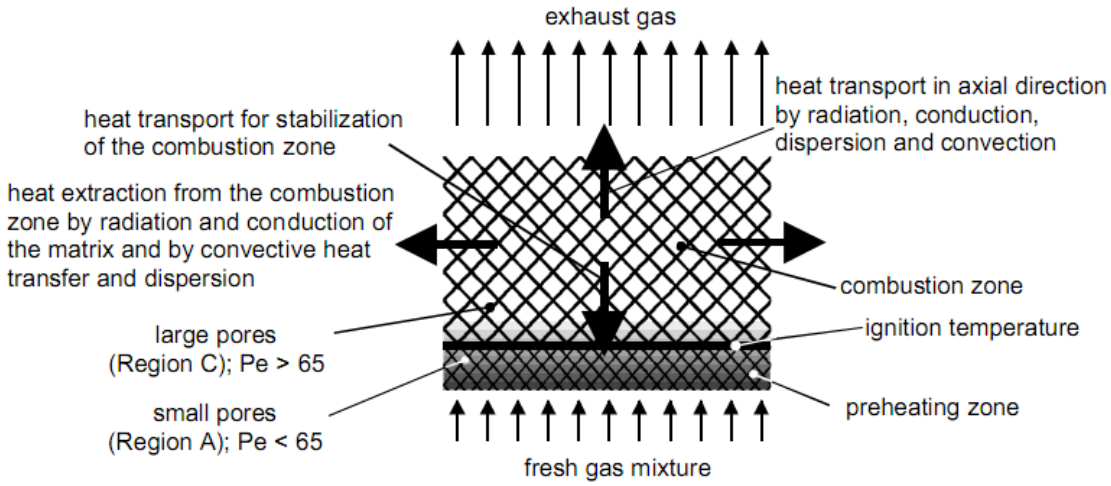

Figure 2.11 Heat transport and flame stabilization in a two-layer porous burner (Trimis et al., 1996).

Brenner et al. (2000) developed the numerical modeling to examine the matrix stabilized methane/air combustion within bi-layered porous inert media. The numerical code is utilizing a pseudohomogeneous heat transfer and flow model for the porous material was used. The 2-Dimensions, 20 species, two momentum equation, and one-energy equation were also considered. In addition, the numerical solutions were validated with the experimental results. The comparison was shown that there was good agreement between the numerical solutions and the experimental data. The developed numerical model study was an excellent tool to simulation combustion phenomena in porous media.

Barra and Ellzey (2004) were defined the heat recirculation and the output radiant efficiency by using a one-dimensional numerical modeling. The burner geometry of bi-layered porous burner was used in this work as shown in Fig. 2.12. The GRI 1.2 chemical kinetics mechanism with 32 species and 177 reactions was represents the chemistry.

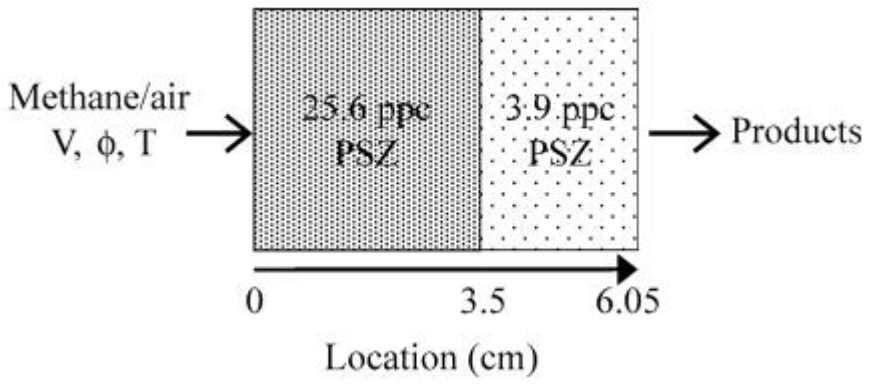

Figure 2.12 Burner geometry (Barra and Ellzey, 2004).

The heat recirculation efficiency was considered the amount of heat transferred to the gas in the preheat zone and was defined as following;

$$\text{Heat recirculation efficiency} = \left[\frac{\text{solid-to-gas convection in preheat zone}}{\text{firing rate}} \right] \qquad (2.13)$$

The output radiant efficiency is defined as

$$\text{Output radiant efficiency} = \left[\frac{\text{output radiation}}{\text{firing rate}} \right] \tag{2.14}$$

The flame structure stabilized in a porous medium at the inlet velocity of 60 cm/s and an equivalence ratio is 0.65 as shown in Fig.2.13. The flame was located between the two sections of porous media (x = 3.5 cm). At the pre-flame zone, prior to the maximum heat release rate, the solid temperature is higher than the gas temperature. Therefore heat was transferred from the hot solid to the incoming gas by solid-to-gas convection prior to combustion. At the downstream from the reaction, the product gas combustion temperature is greater than the solid temperature thus heat is transfer from the gas phase to the solid phase. Precipitously, the hot solid radiates and conducts heat to the solid matrix at the upstream of the flame. Moreover, the results shown that with increasing equivalence ratio, heat recirculation efficiency and the output radiant efficiencies were decreased.

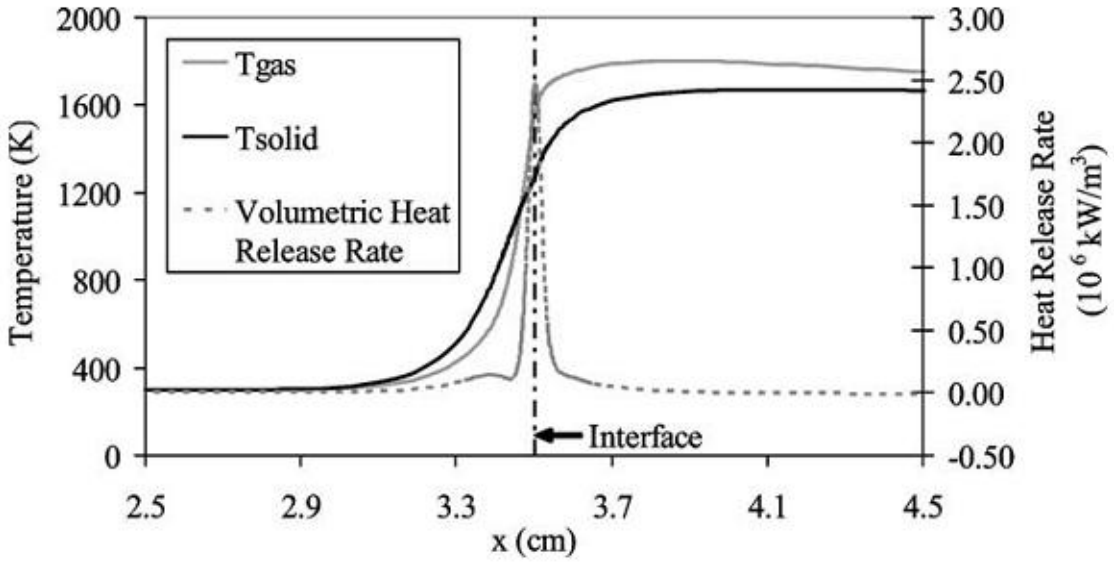

Figure 2.13 Solid and gas temperature and volumetric heat release for inlet gas velocity of 60 cm/s and Φ = 0.65 (Barra and Ellzey, 2004).

Dhamrat and Ellzey (2006) proposed numerical and experimental study of the methane convers to hydrogen via using porous media reactor. The aim of the investigation was to

understand the characteristics of ultrarich propagating combustion waves within an inert reticulated ceramic foam reactor. Also, determine the effect of a number of parameters on methane to hydrogen conversion. The experimental setup consisted of three main systems, which are the flow system, the reactor, and the data acquisition systems (refer to Figure 2.14). The operating condition were examined at the range of equivalence ratios between 1.5 to 5 at a fixed inlet velocity (55 cm/s), which equated to an interstitial velocity of 65.9 cm/s based on a porosity of 0.835. The computational domain for one section reactor is shown in Fig.2.15. The one-dimensional reacting flow, solid-and gas- phase conduction, solid radiation, solid to gas heat transfer, species diffusion, and full chemistry were considered in the model. The conservation equations for mass, gas energy, solid energy, and gas species were solved. The study can be concluded that the predicted conversion efficiency tends to match the patterns recorded from the experimental. The percentage conversion was increased with higher inlet velocity due to the higher peak gas temperature. Moreover, the specific heat of porous media dominated affected the percentage conversion.

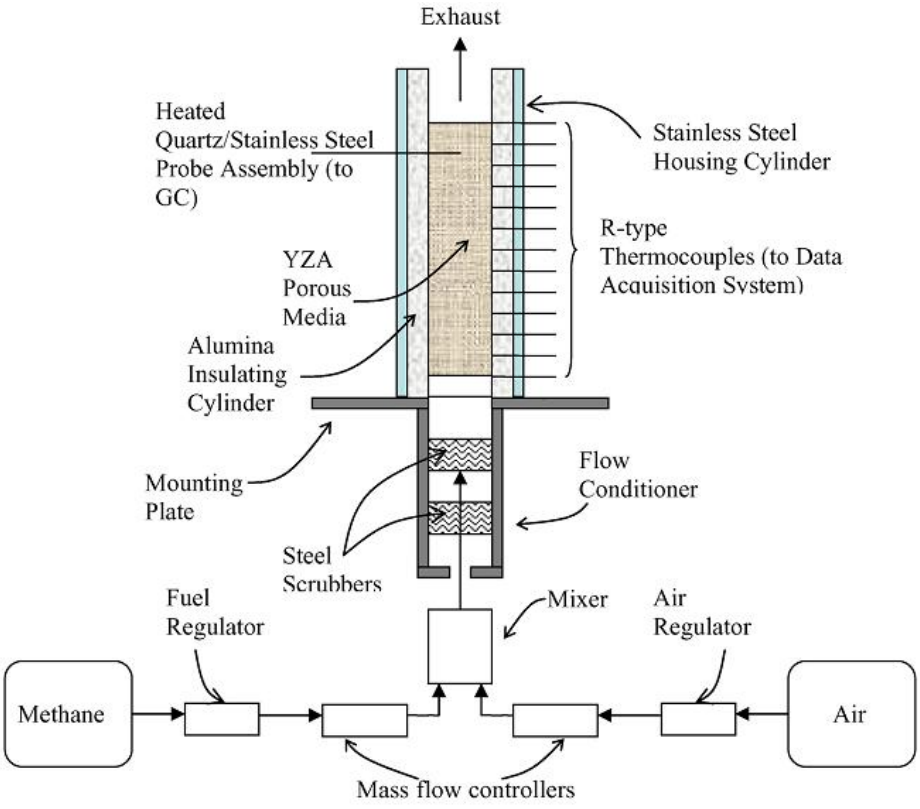

Figure 2.14 Experimental apparatus (Dhamrat and Ellzey, 2006).

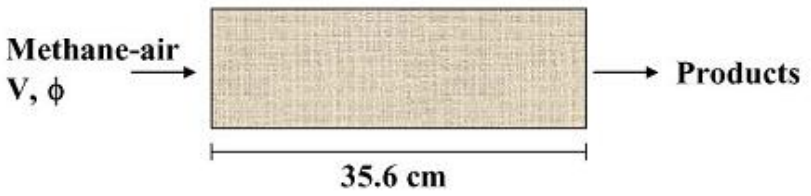

Figure 2.15 Computational domain for one section reactor (Dhamrat and Ellzey, 2006).

Pereira et al. (2010) developed the numerical modeling of methane thermal partial oxidation reforming process within inert porous media, which was validated with experiments. A quasi-1D combustion model with a 12-steps reduced chemistry was applied. The quasi-1D model was supported by preliminary 3D study of the isothermal fluid flow though the full porous solid structure. This model used to provide the realistic cross-sectional area variation of the quasi-1D. The results shown that the 3D/1D coupling concept could be used to simplify the modeling of porous media reactive systems, strongly reducing the computation time for the non-feasible 3D full porous structure with detailed chemistry.

However, previous studies were concerned on the premixed flame within porous inert media burner (PMB). In the premixed flame, fuel and air are early and well mixed at mixing section, thus fuel and air have lots of time for reaction (Levenspiel, 1999). This can cause an undesirable auto-ignition outside the desired location. This makes the premixed flame is less popular in practical applications as compared with the diffusion flame. For the PMB with diffusion flame, only a few studies have been reported. Although the diffusion flame emits more emission, the diffusion flame is safer to operate compared with the premixed flame. In order to the fuel and air flows are separated and unable to react outside the desired location. In other words, the fuel-air mixture in the diffusion flame is late and only occurred at exit leaving (reaction zone). Therefore it is impossible to react before desired location. Moreover, the combustion with diffusion flame is simpler to design because a perfect reactant mixing proportions is not required. Thus, in a large number of industrial combustion systems are using diffusion combustion.

Kamiuto et al. (2004) used a flame sheet model to study characteristic features of flame shapes and flame height of diffusion flames for methane-oxygen in cylindrical and plane-parallel packed beds of the PMB. The experimental study was conducted to estimate the actual flame shapes in the packed bed from upper surface of the packed bed and validate the flame sheet model photographs. Results are illustrated that the flame shapes elongations depend on the properties of the PMB, which are dimension, diameter of sphere and porosity. However, gas and solid temperature, heat recirculation, and radiant output efficiency are eliminated.

Dobrego et al. (2001) developed a two-dimensional, two-temperature, and multi-component model for non-premixed filtration combustion within the PMB, which combined some turbulent diffusion flames properites and premixed filtration combustion. The tubular burner with coaxial feed was considered. The parametric study of radiative efficiency of the PMB was also reported. The model predicted a high flame stability with low equivalence ratios. The results indicated that the Burke-Schumann combustion and mixing rate was well match with the heat release rate in a non-premixed filtration combustion system. However, the heat recirculation in the PMB as well as the validation of simulation model was not analyzed. A classification of analytical studies on porous burners can be summarized in Table2.1.

Moreover, the combustion within the PMB have been described by many research groups (Howell et al.(1996), Trimis and Durst (1996), Kamal et al. (2006), Wood and Harris (2008), and Mujeebu et al. (2009)). In addition, several research groups clarified the reciprocating combustion of premixed gases in PMB both the experimental and numerical (Hanamura and Echigo (1993), Hoffmann et al. (1997), Xie et al. (2009), Jugjai and Sawananon (2004), Jugjai and Nungniyom (2009)). The almost all of the studies have been focused on premixed gaseous fuel porous medium burners. However, the combustion of liquid fuel within porous media has been interested in the small group.

Table 2.3 Reported study on combustion model of PMB.

Reference	Burner	Flame type	Dimension	Combustion model	Validated with experiment	Burner performance indication
Yoshizawa et al. (1988)	SL	premixed	1	single-step	No	flame temperature and flame speed
Tong et al. (1990)	SL	premixed	1	none (localized heat source)	No	flame temperature and radiant output
Sathe et al. (1990)	SL	premixed	1	single-step	Yes	flame temperature, flame speed and radiant output.
Henneke and Ellzey (1999)	SL	premixed	1	Multi-step	Yes	flame temperature
Brenner et al. (2000)	BL	premixed	2	Multi-step	Yes	flame temperature and emission

Table 2.3 continuation

Reference	Burner	Flame type	Dimension	Combustion model	Validated with experiment	Burner performance indication
Barra and Ellzey. (2004)	BL	premixed	1	Multi-step	Yes	Flame temperature, Stability limit, Flame speed, heat recirculation and radiant output efficiency
Raviraj S. Dhamrat and Janet L. Ellzey (2006)	SL	Premixed	1	Multi-step	Yes	Flame temperature, propagation velocity and Hydrogen molar fraction
J.M.C. Pereira et.al. (2010)	SL	Premixed	Quasi-1D	Multi-step	Ys	Flame temperature and Hydrogen molar fraction
Kamiuto and Miyamoto (2004)	SL	Diffusion	2-D	-	Yes	-
Dobrego et al. (2001)	SL	Diffusion	2-D	-	No	Radiative efficiency

2.5 State of liquid fuel combustion using porous media

Liquid fuels are predominated in industrial application because the liquids fuels are easier storage compare with gaseous fuels. However, the liquid fuel combustion is more complicated than gaseous fuel combustion. Liquid fuels must be changed from liquid phase to gas phase before combustion, while gaseous fuel can be ignited and combusted in the normal condition with enough air. The complex phenomenon of liquid fuel combustion with phase change under complex heat transfer is still lack of information.

The vaporizing droplet behavior were described by Kuo (1986), Williams(1985), Glassman (1987), and Turns (2000). There are six types of droplet-vaporization models. In order of increasing complexity, they are (i) constant-droplet-temperature model (which yields the famous d^2 law whereby the square of the droplet diameter or radius decreases linearly with time), (ii) infinite-liquid-conductivity model (uniform but time-varying droplet temperature), (iii) spherically symmetric transient droplet-heating (or conduction-limit) model, (iv) effective-conductivity model, (v) vortex model of droplet heating, and (vi) Navier-Stokes solution. There are various differences among these models, but the essential issue is the treatment of the heating of the liquid phase that is usually the rate-controlling phenomenon in droplet vaporization, especially in high-temperature gases. Some of the models will be shown to be limits of another model (William, 2010).

However, previous studies were allocated with droplet evaporation in the free space. However there are very few papers focused on combustion with phase change of liquid fuel within porous media. Martynenko et al. (1998) developed a one-dimensional mathematical model for a self-sustaining combustion of liquid fuel in a porous inert medium as shown in Fig. 2.16. The fuel droplets were injected via a nozzle and evaporated under a complex heat transfer and then was followed by combustion within the PMB. The complex three modes of heat transfer (convection, conduction and radiation) were considered between three phases: gas, solid and liquid (Fig. 2.17). The heat transfer between gas and solid was assumed to be dominant. Also, the unidirectional characters of heat transfer from gas to liquid and from solid to liquid were assumed. The model considered collision probability to analyze fuel droplet collision and deposition on the PMB. The Arrhenius approach for single-step chemical reaction

of a premixed flame was used. The numerical results tend to match the patterns recorded from the experimental ones. However, the effect of important parameters such as equivalence ratio and firing rate on temperature was not examined.

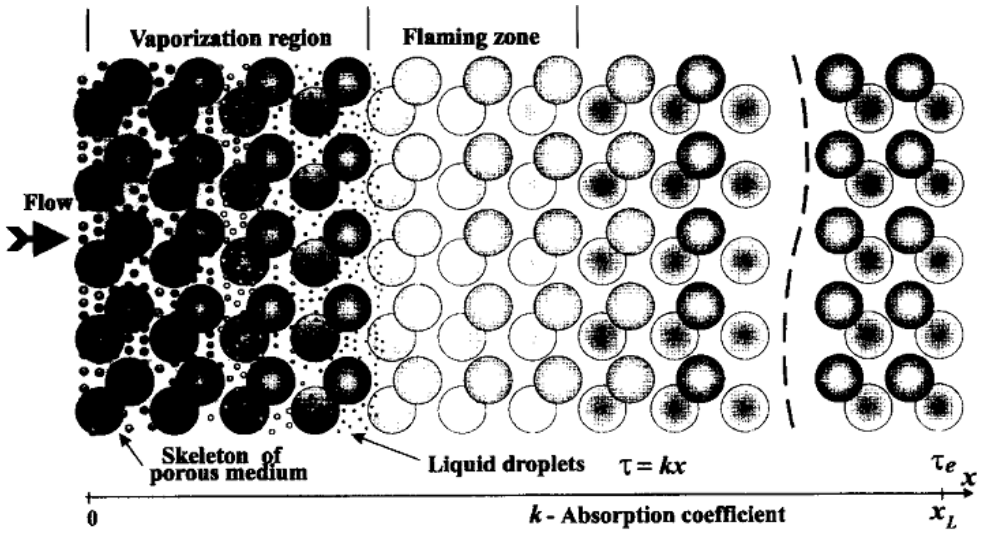

Figure 2.16 Sketch of physical model (Martynenko et al., 1998).

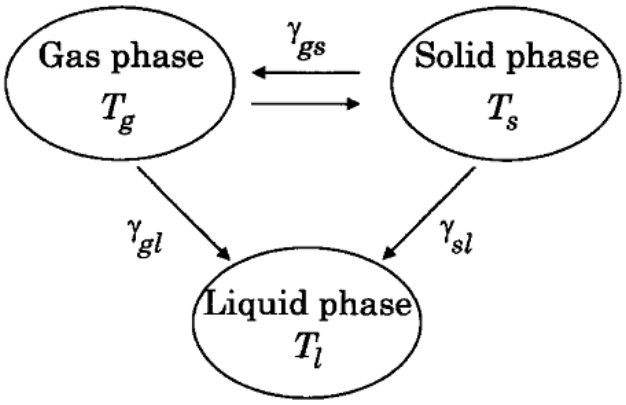

Figure 2.17 Scheme of the most probable convective heat transfer modes between three phases: liquid, gas and solid (Martynenko et al., 1998).

Kayal and Chakravarty (2005) formulated the combustion model of liquid fuel sprayed in a PMB that was made from a porous inert medium as shown in Fig.2.18. The model considered a one-dimension heat transfer. The principal assumptions were complete vaporization of fuel droplets before entering into the flame zone, one-step global irreversible reaction, and no physical interaction between the PMB surface and fuel droplets suspension in the air. The effect of absorption coefficient, emissivity of the

PMB, flame position on radiative energy output efficiency, and optimum oil droplet size at the entry, defined as the maximum size for complete vaporization before entering the combustion zone, were studied. The results show that the PMB with low absorption coefficient provided the high downstream radiative output with large oil droplet sizes. In addition, the numerical study have not validated with the experimental.

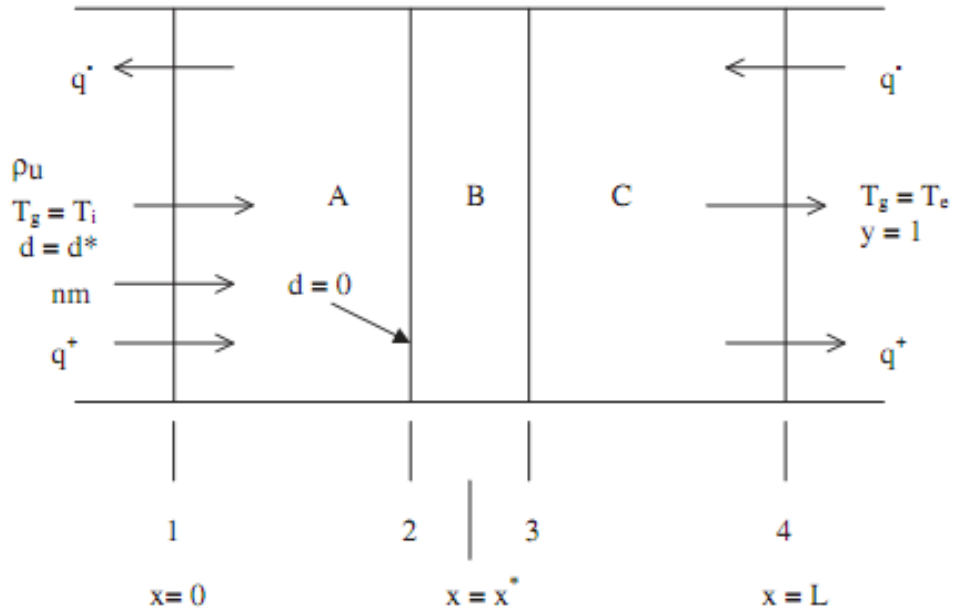

Figure 2.18 Schematic diagram of combustion system in a porous medium (Kayal and Chakravarty, 2005).

Kaplan and Hall (1995) observed the combustion of liquid heptanes within a PMB by experimental study (Fig.2.19). Liquid fuel was sprayed upward on the PMB surface by a pressure atomizer with a fixed flow rate (0.025 lpm) and the fuel droplet diameters in the range of 50-100 μm. Three types of porous inert ceramics, such as magnesia-stabilized zirconia, silicon carbide and yttrium-stabilized zirconia, were used as PMB. A stable and complete combustion occurred with a relatively low CO and NO_x emission. However, the burner operated within a narrow range (equivalence ratios of 0.57-0.67) and the study focused only on heptanes, which has a relatively low vaporization heat. The higher boiling temperature of liquid fuel was not studied in their research.

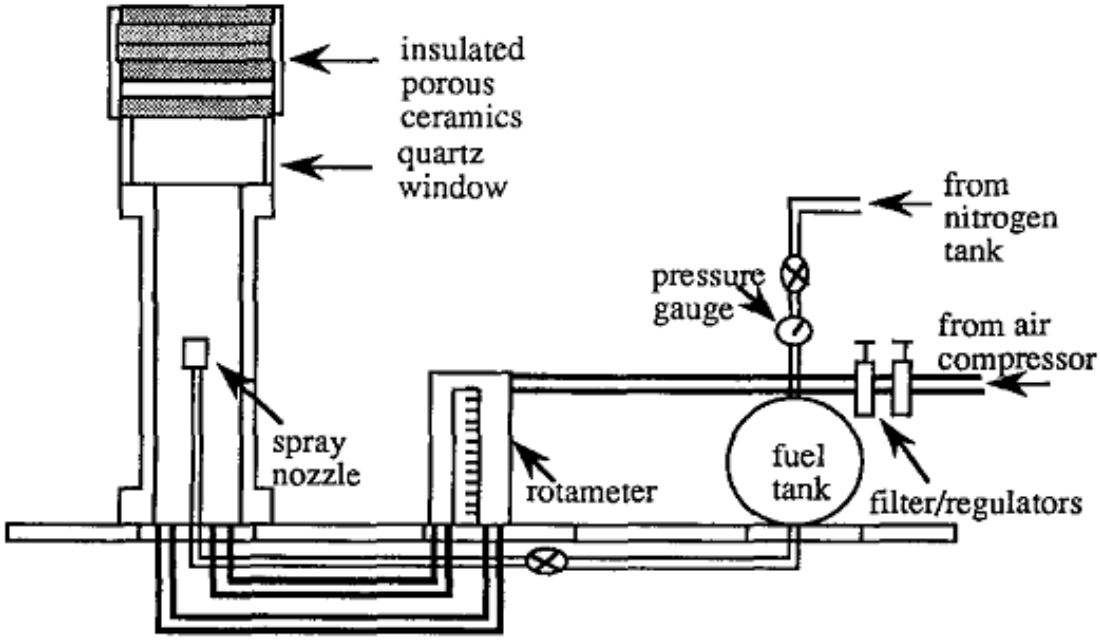

Figure 2.19 Experimental apparatus (Kaplan and Hall, 1995).

As reported in earlier studies, focused on sprayed porous medium burners (PMB), which are complicated for operation system and maintenance. Only a few non-sprayed porous medium burners studies have been reported. Takami et al. (1998) developed a PMB for burning liquid kerosene without atomization. The liquid kerosene was supplied drop-wise to the top of the PMB. At the bottom surface of the PMB, the evaporated kerosene was mixed and burned with a swirling air, which was supplied tangentially from the side wall of the combustion chamber. However, the combustion zone did not occur within the PMB and the temperature profile within it has not been reported. Thus, the evaporation process and the interaction between liquid and solid phase have not been considered.

Tarun and Chakravarty (2006) developed a numerical modeling of trickle flow liquid fuel combustion in inert porous medium. The liquid kerosene was drop through the porous medium under gravity wetting its solid wall with concurrent movement of liquid fuel and air under steady state condition (Fig.2.20). Principle assumptions were one-dimensional heat transfer and single step global reaction mechanism. The investigation of the effects of physical properties of porous medium, operating parameters on vaporization zone and radiant output indicated that ceramic material porous medium

with low emissivity was desirable for maximum downstream and minimum upstream radiative heat loss. However, the numerical results have no experimental validation.

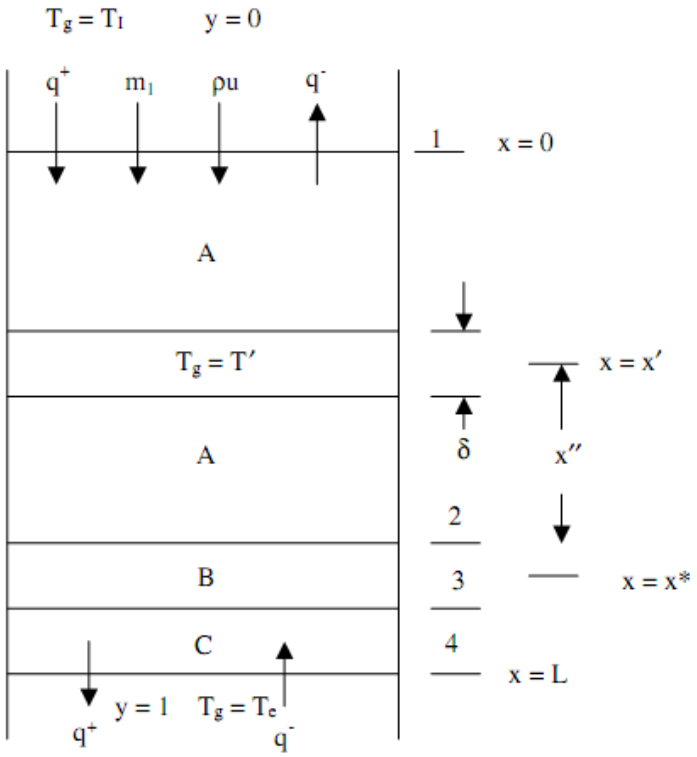

Figure 2.20 Schematic diagram of liquid combustion system in a porous medium (Tarun and Chakravarty, 2006).

Jugjai and Pongsai (2007) proposed a new evaporation and combustion concept of liquid kerosene by using a porous medium burner without atomization, namely, liquid fuel-fired porous burner (LFPB), as shown in Fig.2.21. The liquid fuel was evaporated in an upstream porous matrix, mixed with a swirling air in a mixing chamber, and burned in a downstream porous matrix. Thermocouples positioned along the burner axis in order to monitor the evaporation and combustion zone. The results showed that evaporation within a porous medium followed by a matrix stabilized flame can be achieved. The firing rate effects and equivalence ratio on radiant output efficiency have not been reported. Moreover, the measured temperatures from thermocouples represent the solid temperatures. The liquid and gas temperature in the porous media are difficult to investigated, thus the exact evaporation front and the flame location have not been

elucidated. A numerical modeling is required for further understanding of these phenomena.

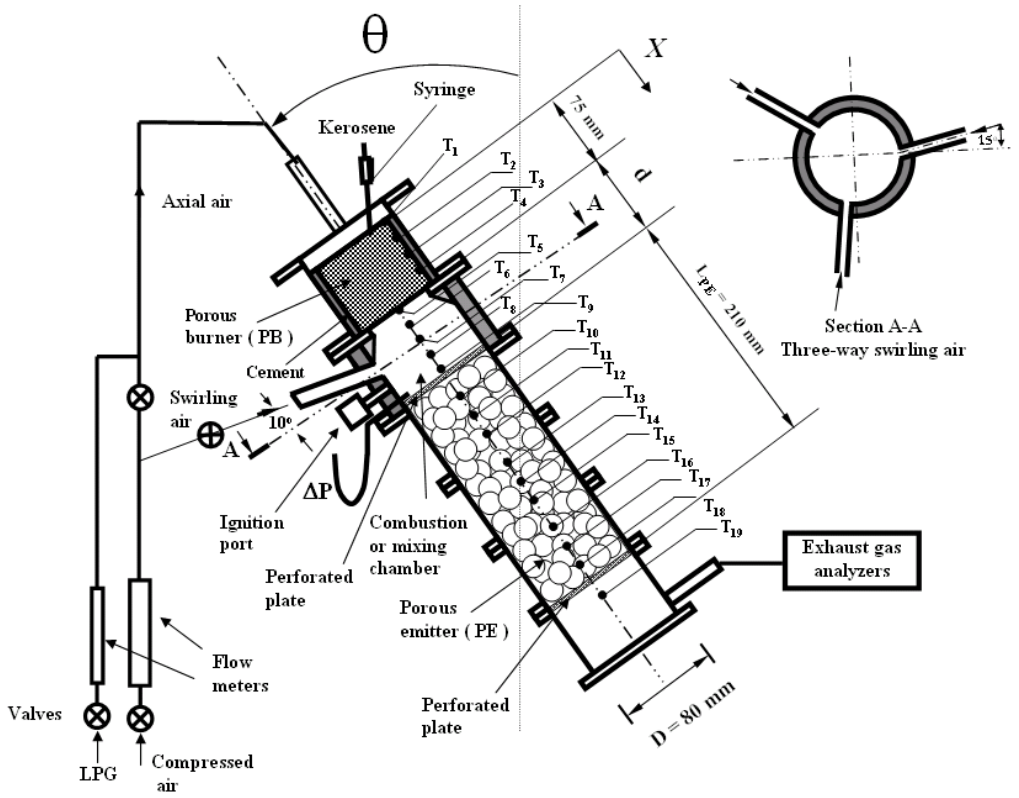

Figure 2.21 Experimental apparatus (Jugjai and Pongsai, 2007).

The current study proposes a new concept of a non-sprayed porous burner (hereafter referred to as NSPB) for burning liquid kerosene. Evaporation followed by combustion within the NSPB is investigated modeling and experimental study. Vaporized fuel and air meet and mix in a mixing chamber in a short time with a late mixing fashion such that a homogeneous combustible mixture of fuel and air. It can be formed using a highly swirling flow motion of the combustion air prior to combustion within the packed bed of the NSPB. The NSPB enhance the air preheating without a risk of undesirable auto-ignition due to the fuel and air are separately introduce through the NSPB, and thus an enhancement in the burner performance can be expected. The numerical model solves liquid, gas and solid phase energy equations for analyzing the evaporation and combustion process. The significant influence of heat transfer between fluid and solid phase, fluid and solid conduction, and solid radiation are also considered. The main parameter affects on the operating conditions such as equivalence ratio and firing rate

on temperature profiles are also monitored. The numerical model validation has been done by comparing experimental results with numerical results and confirms the accuracy of this model.